Lasers in Manufacturing Conference 2015

Surface Structuring by laser remelting of Inconel 718

Andre Temmler[a*], Tobias Schmickler[b], Edgar Willenborg[c]

[a*]*Chair for Lasertechnology, RWTH Aachen University, Steinbachstraße 15, Aachen, 52074, Germany*
[b]*University of Appllied Sciences, Hochschule Koblenz, RheinAhrCampus, Remagen, 53424 , Germany*
[c]*Fraunhofer Institute for Lasertechnology, Steinbachstraße 15, Aachen, 52074, Germany*

Abstract

A new approach of structuring metallic surfaces is structuring by remelting with laser radiation (WaveShape). In this process no material is removed but reallocated while molten. This structuring process is based on the new active principle of remelting. The surface structure and the micro roughness result from a laser-controlled self-organization of the melt pool due to surface tension. Up to now basic research has been focused on hot work steel 1.2343 (AISI: H11) and titanium alloy Ti6Al4V, and promising results have been achieved for this materials. Current research and development is now seeking to expand the spectrum of processable materials. Since remelting is a thermally driven process, significant differences between metals are expected due to their thermos-physical properties such as thermal conductivity, absorption coefficient, viscosity, heat capacity etc.
The nickel based super alloy Inconel 718 has a wide range of industrial applications, especially for turbine components in aviation and aerospace. The innovative WaveShape process for this material will be investigated within this paper. The procedural principle of the WaveShape process is based upon a sinusoidal modulation of laser power while the laser beam is moved over the surface. We used metallographic cross sections to measure the dimensions of melt pool depth and width as they depend on processing parameters, such as laser beam diameter, scanning velocity and laser power. We also investigated basic interdependencies between structural characteristics (e.g. height) and processing parameters used, such as laser beam diameter, laser power, wavelength of modulation and scanning velocity.
The results show that surface structuring by remelting is well suited to process the nickel based super alloy Inconel 718 since structures and process velocities achieved are higher than for the previously investigated hot work steel 1.2343 (H11).

Keywords: surface structuring; Inconel 718; remelting; melt pool; laser surface treatment; material redistribution; no material removal

* Corresponding author. Tel.: +49 241 8906 299; fax: +49 241 8906 121.
E-mail address: andre.temmler@ilt.fraunhofer.de.

1. Introduction

The surface of a part or product strongly influences its properties and functions. Some of these are, e.g. abrasion, corrosion and scratch resistance, haptics as well as the visual impression to the customer. Therefore, many plastic parts have structured surfaces such as leather textures on car dashboards. Usually, these structures are integrated in the injection molds for plastic parts and then transferred to the plastic parts during the injection molding process.

A new approach to structuring metallic surfaces with laser radiation is structuring by remelting ("WaveShape"). In this process no material is removed but reallocated while molten. This structuring process is based on the new active principle of remelting in comparison to the conventional structuring by photochemical etching or structuring by laser ablation, both of which remove material. Surface structure and low micro roughness result from a laser-controlled self-organization of the melt pool due to surface tension.

2. State of the Art

Up to now, there has only been one other structuring process based on a redistribution of material during remelting of the surface. This so-called SurfiSculpt© process is related to structuring by remelting (WaveShape) and was described by Dance & Buxton (Dance and Buxton, 2006). They structured materials by using an electron or laser beam; the process was developed and patented by TWI (The Welding Institute, GB). Within this process an energetic beam is focused on a metallic surface, thereby creating both a melt pool and evaporated material. The focused laser beam is moved with high processing speeds (> 500 mm/s) over the surface to a defined ending point. At the beginning of the remelted track, a hill is created, while at the end of the track, where the energetic beam is turned off, a valley is generated. Since the same track is melted repeatedly, this process is amplified and singular structures comparable to pillars with aspect ratios of up to 30:1 are generated (Blackburn and Hilton, 2011). Generally, all of these singular structures include a hill and a related valley so that a structuring of areas is only possible if by a large number of these structures are combined. So far, an appropriate warmth management of the treated sample seems to be crucial, because in theory identical structures are formed differently with altered distance to one another (Hilton and Nguyen, 2008). In addition, due to throw-offs of the melt pool during processing, the generated structures generally have a rough surface.

Up to now basic research for structuring by remelting (WaveShape) has focused on processing the hot work steel 1.2343 (Temmler, 2012) and Ti6Al4V (Temmler et. al., 2014), and promising results have been achieved for these materials. Current research and development is seeking to expand the spectrum of processable materials. The nickel chromium alloy Inconel 718 has broad spectrum of industrial applications especially in aeronautics. Within this paper we investigate the WaveShape process and not SurfiSculpt©.

3. Set-Up

For surface structuring by remelting (WaveShape) an experimental set-up was used that included a fiber-coupled Q-switch Nd:YAG solid-state laser ($\lambda_{em.}$ = 1064 nm; $P_{L,max}$ = 400 W). The optical set-up mainly serves to project the laser fiber onto the work piece surface (Figure 2). A zoom telescope allows the laser beam diameter to be changed continuously in the range of d_L = 125 µm up to d_L = 800 µm. A 3D laser scanning system enables a fast, three-dimensional deflection of the focused laser beam on the work piece surface.

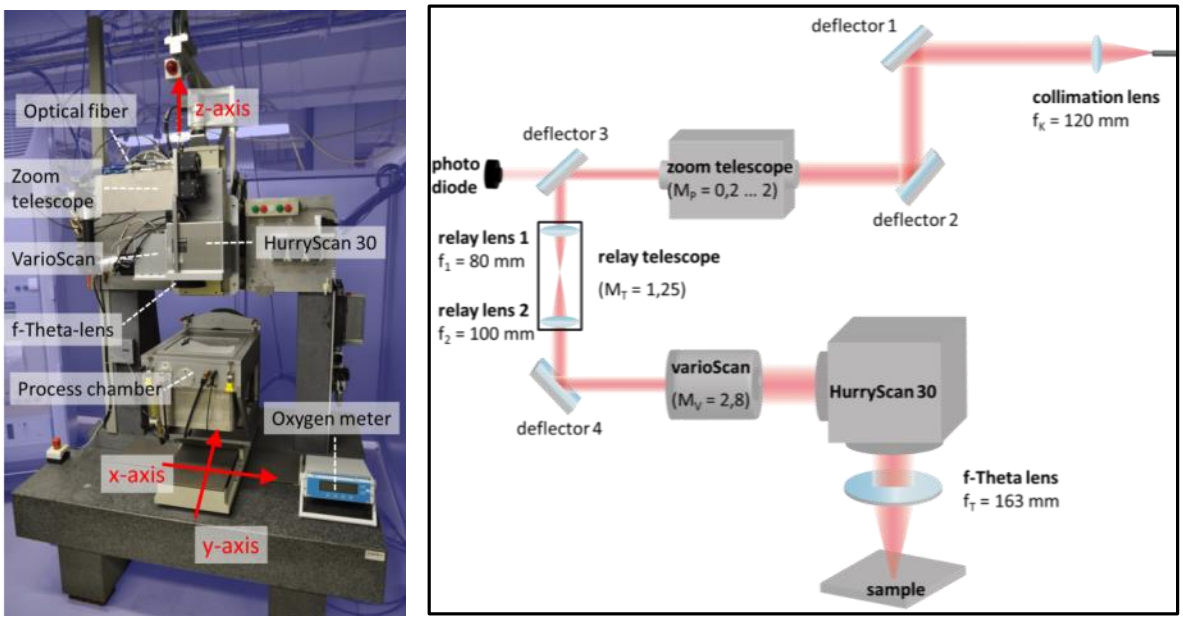

Figure 1: **Left** - Picture of the experimental set-up "Granit-Handling"; **Right** - Schematic diagram of the optical set-up (Temmler et. al., 2014)

During the structuring process, the laser beam can be moved with a velocity of up to 5 m/s and an acceleration of up to 100 g. To focus the laser beam a f-theta-objective was used. Structuring took place in a process chamber, which can be filled with inert gas to avoid unwanted oxidations while the surface is remelted. The remaining oxygen concentration within the chamber was monitored and adjusted to a defined level by an adapted closed-loop control (Temmler, 2012; Willenborg, 2005; Willenborg et. al., 2003). In addition to three "optical" axes for fast laser beam movement, five mechanical axes (three linear and two rotatory) were used for aligning the work piece surface relative to the laser beam. Overall, this experimental set-up can process work pieces with maximum dimensions of 300 x 300 x 100 mm3 using all eight axes. (Temmler et. al., 2014)

4. Process Fundamentals

Surface structuring by laser remelting (WaveShape) is based upon the physical interrelationship between a modulation of melt pool volume and the dependent movement of the three-phase line that determines the resulting surface topography while the molten material solidifies. In laser polishing, changes in the volume of the melt pool are undesirable (Temmler, 2012; Willenborg, 2005; Willenborg et. al., 2003; Temmler et. al., 2009, Ostholt et. al., 2009; Richmann, et. al. 2009, Perry et. al. 2009), but in structuring by remelting, the melt pool volume can be precisely modulated. As a consequence the resulting surface topography is generated by the same mechanism as shown for ripple formation during laser polishing (Pirch et. al., 2006).

Figure 2 left shows the procedural principle of surface structuring by laser remelting. A thin surface layer (< 100 µm) is molten and solidifies afterwards. The direction of the solidification follows the melt pool surface. At constant laser power the melt pool surface is approximately flat and no structuring occurs. An

increase in laser power results in an increase of melt pool volume. Furthermore, density changes from solid to liquid as well as thermal dilatation lead to a bigger volume of the molten material. The melt pool surface is thus bulged outwards. The material becomes structured as the molten material solidifies, following the bulged surface. If the laser power is decreased, the process works exactly the other way around. Therefore, by modulating laser power while a thin surface layer is remelted, structuring can be achieved. (Temmler et. al., 2014)

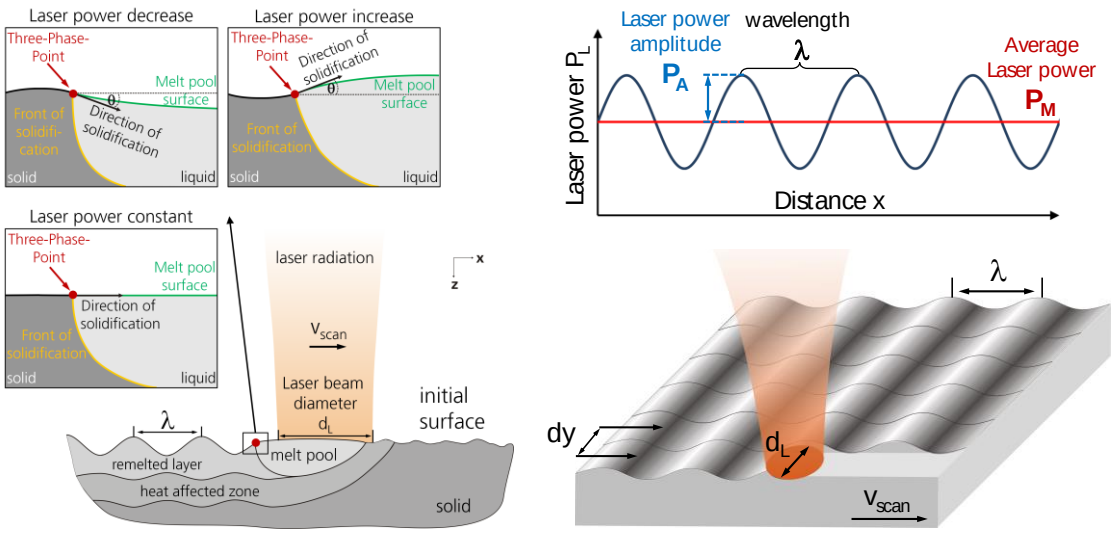

Figure 2: Left - Schematic of the active principle; Right - Schematic of the procedural principle (Temmler et. al., 2014)

A controlled modulation of melt pool volume is essential for structuring by laser remelting. Height, size and form of the produced surface topography depend directly on average melt pool volume, and on the absolute change and time-dependent alteration rate of the melt pool volume. While the average size of the melt pool determines the structural resolution, absolute change and the time-dependent alteration rate of the melt pool volume determine height and symmetry of the produced structures. In order to achieve periodic structures, laser power was modulated sinusoidally at average laser power P_M with an amplitude of P_A and a wavelength λ (Figure 2 right). While the laser power was modulated, the laser beam with diameter d_L was moved unidirectionally over the surface by a 3D laser scanning system at a defined scanning velocity v_{scan} and track offset dy. The wavelength λ of the modulated laser power was equivalent to the wavelength of the remelted structures. In order to obtain compact areas instead of single tracks, an overlap of the remelted tracks was necessary. (Temmler et. al., 2014)

5. Experimental

The main procedural parameters for the WaveShape process are laser power amplitude P_A, laser beam diameter d_L and wavelength of laser power modulation λ. The most important parameter for characterization is structure height h. The interrelationship of laser power amplitude and structure height was investigated as they depend on wavelength, laser beam diameter and number of repetitions. For this purpose, single tracks with a minimum length of six times the wavelength were remelted on a sample made of Inconel 718. The samples are cylindrical with a diameter of 80 mm and flat on both sides. The initial

surface topography for each side of the sample was prepared mechanically by grinding, resulting in an average surface roughness of Sa < 0.1 µm.

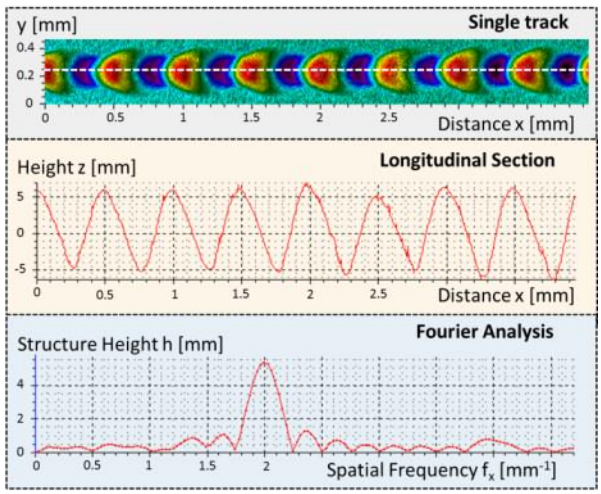

Figure 3: Schematic for single track analysis (Temmler et. al., 2014)

For each set of procedural parameters, five single tracks were structured in order to increase the confidence level. After the single tracks were structured, they were mapped by white light interferometry (Figure 5 top). Based on these measurements, structure height and wavelength of a single track were analysed half-automated along a longitudinal section of the track (Figure 5 middle). An adapted, one-dimensional Fast Fourier Transformation was used; this longitudinal section was analysed in terms of spatial frequencies, phases and corresponding amplitudes (Figure 5 bottom). To precisely determine main spatial frequency and corresponding modulation amplitude, zero-padding is generally used, which leads to a declining ringing effect near the dominant peaks. The spatial wavelength is the inverse of spatial frequency ($\lambda = f^{-1}$), while the amplitude equals structure height h. (Temmler et. al., 2014)

6. Results and Discussion

6.1. Determination of average laser power and laser power amplitude

Depending on laser beam diameter dL and scanning velocity vscan, the maximum laser power amplitude is limited. On the one hand, the minimum laser power is given by the threshold, where the material starts to melt, P_{melt}. On the other hand, the maximum laser power constitutes the ablation threshold, where the material begins to vaporize, P_{vap}. Theoretically, laser power scales linearly with laser beam diameter dL and scanning velocity vscan [1] if the energy per area is kept constant. Therefore, minimum laser power $P_{melt,i}$ and maximum laser power $P_{vap,i}$ were identified for several combinations i of d_L and v_{scan} and their linear interdependencies were verified experimentally. Visible remelting tracks and evaporation of material are criteria which are both robust and easy to handle for determining process limits.

Based on Formulas 1 and 2, average laser power $P_{M,i}$ and maximal laser power amplitude $P_{A,max,i}$ were calculated for each set of procedural parameters investigated after P_{melt} and P_{vap} were identified.

$$P_{M,i} = \frac{P_{vap,i} + P_{melt,i}}{2} \quad (1) \qquad P_{A,max,i} = \frac{P_{vap,i} - P_{melt,i}}{2} \quad (2)$$

Table 1 shows average laser power P_M and maximal laser power amplitude $P_{A,max}$ in dependence on scanning velocity vscan for three laser beam diameters, d_L = 125 µm, d_L = 250 µm and d_L = 500 µm.

Table 1: Processing Parameters P_M and P_A in dependence on d_L and v_{scan}.

d_L [µm]	v_{scan} [mm/s]	P_M [W]	$P_{A,max}$ [W]
125	25	46.25	23.75
	50	52.5	27.5
	100	62.5	32.5
250	25	87.5	42.5
	50	97.5	47.5
	100	117.5	57.5
	200	150	75
500	25	167.5	82.5
	50	192.5	97.5
	75	*219.5*[1]	*110.5*[1]
[1]Calculated values by linear fit			

The values measured for $P_{M,i}$ und $P_{A,max,i}$ show a linear dependency on scanning velocity v_{scan}. For a combination of d_L = 500 µm and v_{scan} = 75 mm/s, the maximal laser power P_{vap} could not be identified because maximal laser power ($P_{L,max}$ = 400 W) of the laser beam source was limited. The values measured for the procedural parameters shown in Table 1 are the basis for the further investigations.

6.2. Influence of laser power amplitude, scanning velocity and wavelength on structure height

To investigate to which extent structure height h depends on laser power amplitude P_A, the laser power amplitude was varied in five equidistant steps according to Formula 3. This was carried out for d_L = 250 µm and v_{scan} = 50 mm/s. The effect was investigated for four distinct wavelengths: λ = 0.5 mm, 1 mm, 2 mm and 4 mm. After the piece was structured, a digitized longitudinal section of each single track was analyzed.

Figure 4 left shows measured values of the structure height and the results of linear regression analysis for the structure height in dependence on P_A for each wavelength. The structure height scales linearly with increasing laser power amplitude P_A The increase of structure height as it depends on laser power amplitude is the biggest for λ = 1 mm and becomes smaller for bigger wavelengths. This is a result of increased laser power gradients for smaller wavelengths.

The influence of wavelength and scanning velocity v_{scan} on structure height was also investigated. Therefore, both P_M und $P_{A,max}$ were adapted to scanning velocity as shown in Table 1. The wavelength was varied as a multiple of the doubled laser beam diameter. The scanning velocity was altered systematically in four discrete steps by successive doubling.

Figure 4 right shows structure height in dependence on wavelength for d_L = 250 µm and v_{scan} = 25, 50, 100 and 200 mm/s. The dynamics of the laser beam source are limited by the time the laser power requires to rise and fall to its maximum, while avoiding evaporation, down to its minimum required to create a melt pool. If processing frequency $f_{pro} = v_{scan} \cdot \lambda^{-1}$ equals or exceeds 100 Hz, the effective output laser power amplitude $P_{A,eff}$ is reduced as compared to the nominal laser power amplitude $P_{A,nom}$ (e.g. for f_{pro} = 100 Hz: $P_{A,eff} \approx 80\ \% P_{A,nom}$). The structure heights for process frequencies $f_{pro} \geq 100$ Hz are marked with circles.

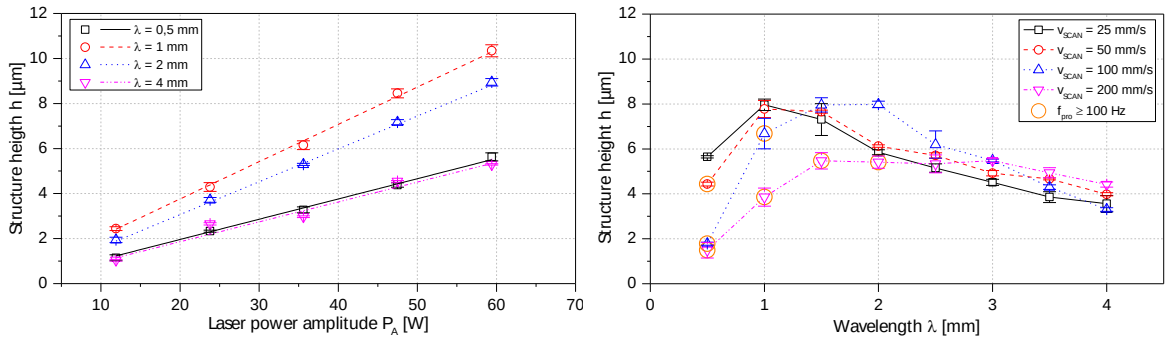

Figure 4: **Left** - Structure height h in dependence on laser power amplitude P_A for four wavelengths λ (P_M = 97.5 W, d_L = 250 µm, v_{scan} = 50 mm/s); **Right** - Structure height h in dependence on wavelength λ for four scanning velocities v_{scan} (P_M and P_A adapted to v_{scan})

The maximum structure height at λ = 1 mm and v_{scan} = 25 mm/s (or v_{scan} = 50 mm/s) is h ≈ 8 µm and decreases to h ≈ 3.5 µm at λ = 4 mm. If the wavelength was smaller than four times the laser beam diameter, a significantly smaller structure height was observed (h ≈ 5.5 µm at λ = 0.5 mm and v_{scan} = 25 mm/s). This decrease in structure height cannot be explained by reduced laser amplitude, but is presumably caused by the ratio of melt pool dimensions and wavelength. For λ = 1 mm, structuring at full laser power amplitude could only be achieved at v_{scan} = 25 mm/s and v_{scan} = 50 mm/s. If v_{scan} is increased to 100 mm/s, structure height drops to h ≈ 6.7 µm due to the reduced effective laser power amplitude. The maximal structure height furthermore was achieved at bigger wavelengths. This was also observed by using a scanning velocity of v_{scan} = 200 mm/s.

As an overall result, structure height is virtually independent of scanning velocity for constant wavelengths λ as long as process frequencies are lower than 100 Hz. Furthermore, the results shown in Figure 4 right indicate that even greater structure heights might be achieved if a laser beam source with shorter times for rise and fall of laser power is used. This corresponds to the results achieved for Ti6Al6V (Temmler et. al.,2014) and 1.2343 (Temmler, 2012).

6.3. Influence of laser beam diameter and scanning velocity on structure height

In order to investigate the influence of laser beam diameter on wavelength-dependent structure height, laser beam diameter was doubled from d_L = 125 µm to d_L = 500 µm. The resulting structure height was investigated in dependence on eight different wavelengths. Again the wavelength was varied as a multiple of the doubled laser beam diameter.

Figure 5 left shows a comparison of structure heights achieved as they depend on wavelength, using three different laser beam diameters and three different scanning velocities. For d_L = 500 µm, maximal structure height was h ≈ 16 µm at λ = 2 mm and declined to h ≈ 18 µm at λ = 6 mm. If the wavelength was smaller than four times the laser beam diameter, a significant smaller structure height was observed (h ≈ 7 µm at λ = 1 mm and v_{scan} = 75 mm/s). Maximal structure height was achieved at a wavelength that is two times the wavelength as it is for d_L = 250 µm (h ≈ 8 µm at λ = 1 mm). The greatest structure heights were achieved using the smallest scanning velocity of v_{scan} = 25 mm/s and were reduced up to 20% for wavelengths from λ = 2 mm up to λ = 5 mm at v_{scan} = 100 mm/s.

The increase of structure height at a larger laser beam diameter resulted from a larger volume of the melt pool, which allowed a redistribution of more material. When wavelength was normalized to the laser beam diameter ($\lambda_{dL} := \lambda \cdot d_L^{-1}$), the maximum structure height was achieved for all three laser beam diameters at

the same normalized wavelength, $\lambda_{dL} = 4$. In this regard, the observations are consistent with those for tool steel 1.2343.

To directly compare a wavelength-dependent change in structure height, while varying scanning velocity at different laser beam diameters ($d_L = 125$ µm, $d_L = 250$ µm and 500 µm), the relative structure height h_m was plotted versus wavelength, which was normalized to the laser beam diameter $\lambda_{dL} := \lambda \cdot d_L^{-1}$ (Figure 5 right). The relative structure height h_m was calculated as the ratio of structure height h and maximal structure height h_{max} for each combination of scanning velocity v_{scan} and laser beam diameter d_L. The process frequency was smaller than 100 Hz for all sets of procedural parameters plotted in Figure 5 right.

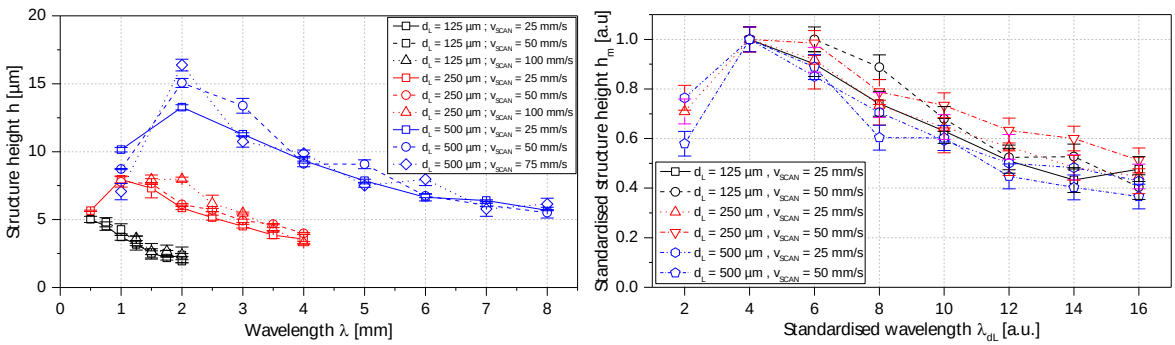

Figure 5: **Left** - Structure height h in dependence on wavelength λ for three scanning velocities v_{scan} and three laser beam diameters d_L (P_M und $P_{A,max}$ adapted to d_L and v_{scan}); **Right** - Standardized structure height h_m as function of standardized wavelength λ_{dL} (P_M and P_A adapted to v_{scan} and d_L)

The biggest standardized structure height h_m can be observed at a wavelength four times the laser beam diameter. The smallest relative structure heights were achieved for a wavelength that is sixteen times the corresponding laser beam diameter, and is $h_m \approx 0.45 \pm 0.1$. Within the error, standardized structure heights decreased linearly for wavelengths larger than $4 \cdot d_L$. This is virtually independent of scanning velocity and laser beam diameter used. The slope of the descending h_m is approximately 5 % per standardized wavelength. That means for wavelengths $\lambda_{dL} > 4$ structure height decreases by approx. 5 % if λ_{dL} is increased by one.

6.4. Structure height in dependence on number of repetitions and wavelength

As previous results show, the achieved structure height was limited up to $h \approx 16$ µm for a large laser beam diameter, maximal laser power amplitude and adapted wavelength of sinusoidal laser power modulation. In order to achieve greater structure heights, the additive effect of a repeated processing with constant procedural parameters, such as P_M, P_A, v_{scan}, d_L and λ was investigated. For this a remelted single track was processed several times, or n, with identical laser power modulation and scanning direction. To quantify the dependency of structure height on repetitions using constant procedural parameters, the number of repetitions was varied systematically from $n = 2^0$ up to $n = 2^6$ in seven steps by successive doubling. While the processing parameters $P_M = 97.5$ W, $P_A = 47.5$ W, $v_{scan} = 50$ mm/s and $d_L = 250$ µm were kept constant, the wavelength was varied systematically in five steps from $\lambda = 0.5$ mm up to $\lambda = 4.0$ mm by successive doubling.

Figure 6 shows structure height h_λ as a function of repetitions n for different wavelengths λ. For small wavelengths in comparison to the laser beam diameter such as $\lambda = 0.5$ mm, almost no further increase in

structure height was achieved by repeating the structuring process. For all wavelengths $\lambda > 1.0$ mm a significant increase in structure height was observed with increasing number of repetitions n. Every additional time the surface was remelted using the same procedural parameters, the height of the structures grew to nineteen times the height achieved after remelting only once. Thus, the quantity of increase depends strongly on the wavelength used and does not scale linearly with the number of repetitions.

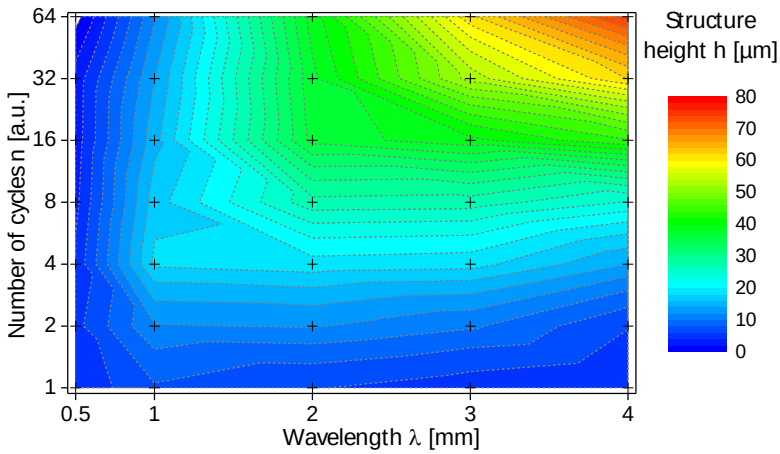

Figure 6: Structure height as a function of repetitions n for different wavelengths λ. (P_M = 97.5 W, P_A = 47.5 W, v_{scan} = 50 mm/s and d_L = 250 µm)

6.5. Metallographic characteristics of remelted tracks and comparison of results for Inconel 718, 1.2343 and Ti6Al4V

Figure 7 left shows a micrograph of a remelted track on a ground surface of Inconel 718. The micrograph represents the typical appearance of a single track remelted with constant laser power. The remelted material differentiates itself clearly from the initial, ground surface by sharp edges. Within the remelted track, a microstructure is visible that is characteristic for the nickel chromium alloy.

At the border of the remelted tracks to the initial material a characteristic area of fine grains was created. Due to different grain size, growth and orientation, a micro roughness on the remelted surface was created.

The main characteristics of remelted single tracks are width and depth of the remelted material. The size of remelting depth and width was evaluated and measured by micrographs of cross-sections of single tracks. Each single track was remelted at constant laser power. The length of each track was 20 mm and the track was cut in the middle, between starting and end point. A typical micrograph of a cross-section for a remelted track on Inconel 718 is shown in Figure 7 right. The dimensions of the remelted track and the homogenized surface are marked in green and orange, respectively. Since the size of the melt pool presumably has a significant influence on the resulting structure height, both width and depth of the remelted tracks were measured and compared to 1.2343 and Ti6Al4V. Additionally structure heights achieved for these materials were compared using the same procedural parameters.

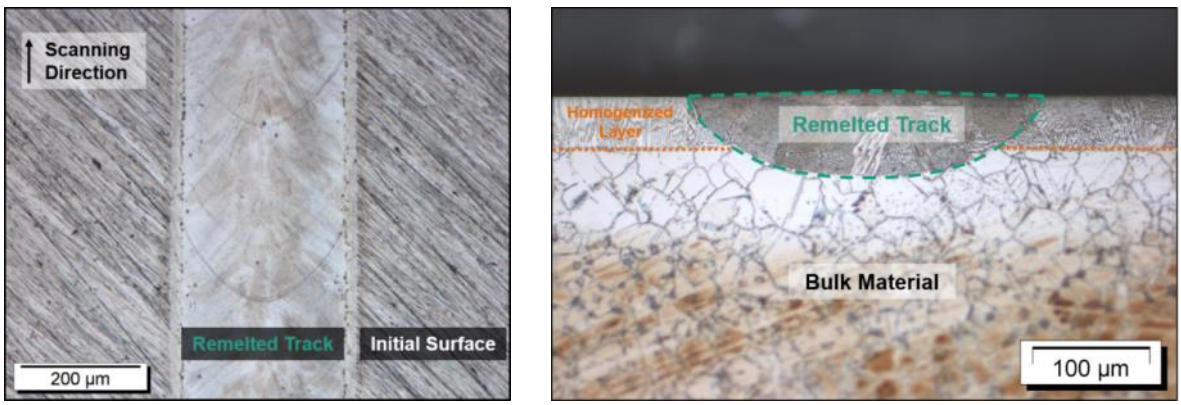

Figure 7: Left - Micrograph of a remelted track on a ground surface of Inconel 718 (Onsight); Right - Micrograph of cross-section of a remelted track on a Inconel 718 surface (right); (d_L = 250 µm, v_{scan} = 100 mm/s, P_L = 125 W)

Figure 8 left shows the dimensions of the remelted track in terms of width and depth as a function of laser power for Inconel 718 in comparison to 1.2343 and Ti6Al4V. The width and depth of the remelted track are significantly bigger for Inconel than for 1.2343, while the process limits for both materials are in the same region. For In718 laser power was varied from P_{min} = 50 W up to P_{max} = 145 W, for 1.2343 it was varied from P_{min} = 65 W up to P_{max}=155 W, whereas for Ti6Al4V the laser power was varied from P_{min} = 50 W up to P_{max} = 180 W, without ablating material and using the same laser beam diameter d_L = 250 µm and scanning velocity v_{scan} = 50 mm/s. As can be seen in Figure 8 left, there is a significant difference in the size of the remelted tracks when both materials are compared. For example, at P_L = 120 W the width and depth for Inconel 718 are w_{IN718} = 383 ± 6 µm and d_{IN718} = 98 ± 3.5 µm, whereas the dimensions for 1.2343 are $w_{1.2343}$ = 282 ± 9 µm and $d_{1.2343}$ = 59 ± 5 µm, respectively, and for Ti6Al4V are w_{Ti64} = 400 ± 13 µm and d_{Ti64} = 130 ± 7 µm.

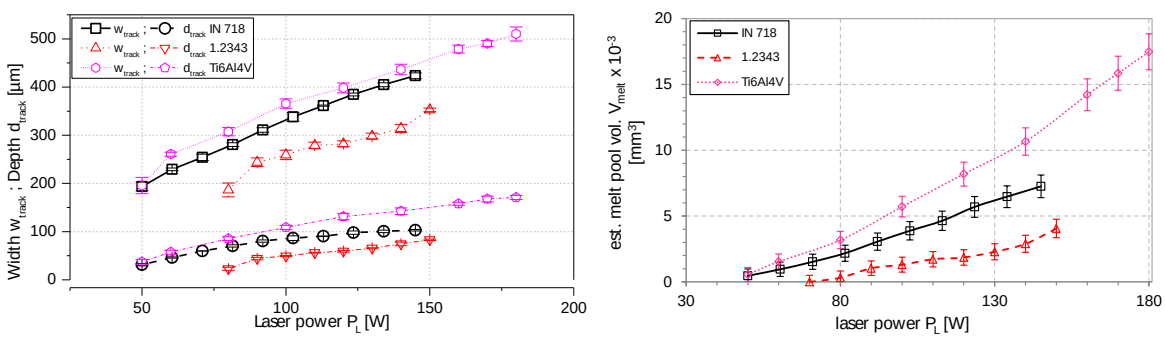

Figure 8: **Left** - Size of remelted track as function of laser power P_L for Inconel 718, 1.2343 and Ti6Al4V (d_L = 250 µm, v_{scan} = 50 mm/s); Right – Estimated melt pool volume as function of laser power for Inconel 718, 1.2343 and Ti6Al4V. Data for materials 1.2343 and Ti6Al4V taken from (Temmler, 2014).

Based on this data for melting width and depth for these materials the melt pool volume was roughly estimated in dependence on laser power. Therefore, the base area of the melt pool was estimated to be circular with a radius of the size that equals half of the width. The phase front between molten and solid material within the bulk material has a rather complex shaped geometry and cannot be measured properly after the

remelting process. Therefore the melt pool volume is simplified to a cylindrical shape. The measured remelting depth is estimated to contribute half to the volume of the melt pool. Therefore, melt pool volume is estimated to be $^{\pi}/_{4} \cdot \text{width}^2 \cdot {}^{1}/_{2} \cdot \text{depth}$. The estimated melt pool volume V_{melt} in dependency on laser power for Inconel 718, 1.2343 an Ti6Al4V is shown in Figure 8 right. The estimated melt pool volume for Inconel 718 lasts from $V_{melt} = 0.46 \pm 0.33 \cdot 10^{-3}$ mm^3 at $P_{L,\,min} = 50$ W to $V_{melt} = 7.25 \pm 0.87 \cdot 10^{-3}$ mm^3 at $P_{L,\,max} = 145$ W, whereas the estimated melt pool volume for 1.2343 lasts from $V_{melt} = 0.31 \pm 0.21 \cdot 10^{-3}$ mm^3 at $P_{L,\,min} = 65$ W to $V_{melt} = 4.06 \pm 0.71 \cdot 10^{-3}$ mm^3 at $P_{L,\,max} = 150$ W and for Ti6Al4V it lasts from $V_{melt} = 0.56 \pm 0.31 \cdot 10^{-3}$ mm^3 at $P_{L,\,min} = 50$ W to $V_{melt} = 17.48 \pm 1.38 \cdot 10^{-3}$ mm^3 at $P_{L,\,max} = 180$ W. The dependency of melt pool volume on laser power is virtually linear as can be expected from theory. Nonetheless, the slope of melt pool expansion as function of laser power strongly depends on material properties, especially thermo-physical properties such as thermal conductivity, absorption coefficient, viscosity, heat capacity etc.

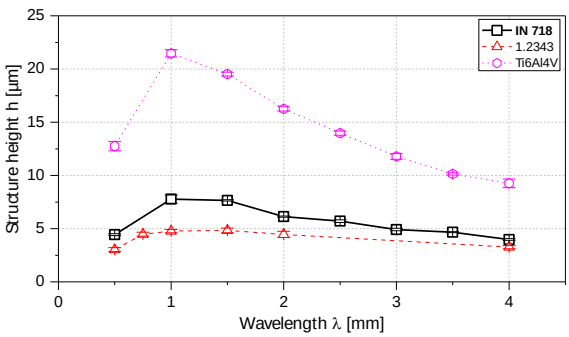

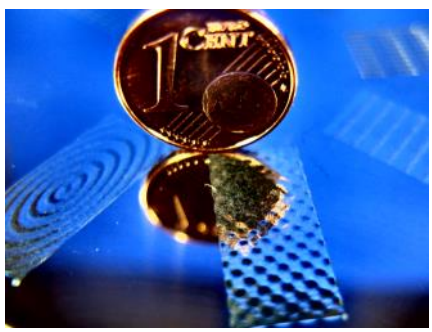

Figure 9: **Left** - Comparison of structure height as a function of wavelength for Inconel 718, 1.2343 and Ti6Al4V ($d_L = 250$ µm, $v_{scan} = 50$ mm/s, $P_M = 110$ W and $P_A = 50$ W). Data for materials 1.2343 and Ti6Al4V taken from (Temmler, 2014).
Right – Photograph of some periodic structures on Inconel 718 produced with the WaveShape process.

Figure 8 right shows a comparison of structure height as a function of wavelength for the materials Inconel 718, 1.2343 and Ti6Al4V. When 1.2343 and Ti6Al4V were structured ($d_L = 250$ µm, $v_{scan} = 50$ mm/s, $P_M = 110$ W, $P_A = 50$ W, n=1), the greatest structure height was achieved for these materials at a wavelength that equals four times the laser beam diameter. Maximum structure height for Inconel 718 is approx. 8 µm, whereas the height for 1.2343 is approx. 5 µm and for Ti6Al4V it is approx. 22 µm. These maximum heights after one structuring cycle were achieved for each material at $\lambda = 1$mm.

7. Summary & Outlook

Surface structuring by remelting constitutes a new approach to structuring metallic surfaces with laser radiation. In this process no material is removed but reallocated while molten. It has been shown that the structure height depends linearly on the laser power amplitude, which is used for a sinusoidal modulation of laser power while structuring Inconel 718. Furthermore, the achieved structure height is not dependent on scanning velocity if laser power is adapted linearly to scanning velocity. However, a limiting factor for structuring is the process frequency, which depends on the dynamics of the laser beam source. Maximal structure heights are generated for structures at wavelengths $\lambda = 4 \cdot d_L$ for Inconel 718 as well as for hot work steel 1.2343 and Ti6Al4V. An increase of laser beam diameter results in an approximately linear increase of structure height, as long as average laser power and laser power amplitude are adapted to the laser beam diameter. The increase in structure heights results from bigger melt pool volumes that are

created with greater laser power and laser beam diameter. However, the increase in structure height is accompanied by an increase in minimal wavelength, at which maximal structure height is achieved. An interesting scientific question remains: whether this results directly from the physical interrelationship of laser beam and material by thermal flow and heat conduction or if it is also influenced by the dynamics of the laser beam source. Until now it seems to be independent of the material used, but that has to be further verified for additional materials. For all wavelengths $\lambda \geq 4 \cdot d_L$ a significant increase in structure height is observed as the number of repetitions n increases. Every additional time the surface is remelted using the same procedural parameters, the height of the structures grows up to ten times the height achieved after remelting only once. Thus, the quantity of increase depends strongly on the wavelength used and does not scale linearly with the number of repetitions.

An analysis of remelting depth and width showed that the melt pool dimensions have significant influence on the resulting structure height. Nevertheless, additional effects on the structure height ae assumed to have an influence, such as time-dependent gradient of laser power and plastic deformation, have to be investigated in the future.

So far, essential procedural parameters of the structuring by remelting have been identified, and periodic structures have been attained for Inconel 718 (Figure 9 right). Using an adapted space-resolved modulation of laser power, we have shown that multiple, novel and complex structures can be structured on flat surfaces. As seen within this paper, the spectrum of processable materials could be expanded to Inconel 718. The results show a good suitability of Inconel 718 for structuring by remelting since structures and process velocities we achieved are higher than for those previously investigated hot work steel 1.2343.

The next steps we plan to carry out are additional experimental investigations for other materials to expand the material spectrum for structuring by remelting even further and to derive finally essential interrelationships between procedural parameters, material properties and achieved structures. Therefore, additional materials, such as ball bearing steel 100Cr6, cobalt alloy CoCr28Mo and stainless steel 1.4301 will be investigated within the research project “WaveShape” sponsored by the Volkswagen Stiftung.

Acknowledgements

This work has been partially funded by the Volkswagen Foundation and German Federal Ministry for Education and Research (BMBF). We like to thank the Volkswagen Stiftung for their generous sponsorship of the research project “WaveShape.” Also we would like to thank the BMBF for their generous sponsorship of the research project “EffiLas.” The results above were acquired partially using facilities and devices funded by the Federal State of North-Rhine Westphalia within the Center for Nanophotonics under grant number 290047022.

References

Dance, B.G.I., Buxton, A.L. (2006) Surfi-Sculpt - A new Electron Beam Processing Technology, In Proceedings of 8th International Conference on Electron Beam Technologies, Varna.

Blackburn, J., Hilton, P. (2011) Producing Surface Features with a 200W Yb-fibre Laser and the Surfi-Sculpt Process, in Proceedings of the 6th International WLT-Conference on Laser in Manufacturing. Munich, Germany, 529-536.

Hilton, P., Nguyen, L. (2008) A new method of laser beam induced surface modification using the Surfi-Sculpt process, in Proceedings of the 3rd International Conference on Application of Lasers and Optics, Beijing, China.

Temmler, A. (2012) Laserumschmelzstrukturierung, Ph.D. thesis, RWTH Aachen, Germany, Shaker Verlag.

Temmler, A., Walochnik, M.A., Willenbog, E., Wissenbach, K. (2014), Surface Structuring by laser remelting of titanium alloy Ti6Al4V, in Proceedings of the 33rd International Congress on Applications of Lasers & Electro-Optics (ICALEO®), San Diego, USA, pp. 713-722.

Willenborg, E. (2005) Laserpolieren von Werkzeugstählen, Ph.D. thesis, RWTH Aachen, Germany, Shaker Verlag.

Willenborg, E., et al. (2003) Polishing by laser radiation, in Proceedings of the 2nd Int. WLT-Conference on Lasers in Manufacturing, Munich, Germany.

Temmler, A., et al (2009) Structuring by Remelting, in Proceedings of the 5th Int. WLT-Conference on Lasers in Manufacturing, Munich, Germany.

Ostholt, R., et al (2009) Laser polishing of freeform surfaces, in Proceedings of the 5th Int. WLT-Conference on Lasers in Manufacturing, Munich, Germany.

Richmann, A., et al (2009) Laser polishing of fused silica, in Proceedings of the 5th Int. WLT-Conference on Lasers in Manufacturing, Munich, Germany.

Perry, T.L. et al (2009) Pulsed laser polishing of micromilled Ti6Al4V samples, Journal of Manufacturing Processes (2009).

Pirch, N. et al (2006) Mechanisms of surface rippling during laser polishing, in Proceedings of the 8th Int. Seminar on Numerical Analysis of Weldability, Graz-Seggau, Austria.

Temmler, A., et al (2011) Design surfaces by laser remelting, in Proceedings of the 6th Int. WLT-Conference on Lasers in Manufacturing, Munich, Germany, 419-430.